

**MORPHOLOGIC MAP OF GLACIAL AND PERIGLACIAL FEATURES IN THE NORTHWESTERN ARGYRE BASIN, MARS.** J. Raack<sup>1</sup>, H. Hiesinger<sup>1</sup> and D. Reiss<sup>1</sup>, <sup>1</sup>Institut f. Planetologie, Westfälische Wilhelms-Universität, Wilhelm-Klemm-Str. 10, 48149 Münster, Germany, [jan.raack@uni-muenster.de](mailto:jan.raack@uni-muenster.de)

**Introduction:** Previous studies of morphologic features in the Argyre Basin suggested that they could have been formed by glacial processes [1,2,3]. Based on crater counts, Kargel et al. [1] concluded that the glaciation occurred within the Amazonian about 2.3 – 0.25 Ga ago. This is in agreement with the age (~0.4 Ga) presented by Banks et al. [3], which is based on High Resolution Imaging Science Experiment (HiRISE) imagery. Possible evidence for a past glaciation of the Argyre basin include landforms interpreted as e.g., eskers, drumlins, moraines and kettles [1]. Lobate debris aprons interpreted as rock glaciers [4] surround numerous mountains in the Argyre basin [1]. Glacial features like lineated grooves, stream-lined hills, U-shaped valleys and semicircular embayments (possible cirques) are consistent with extensive glacial modifications in the Argyre Basin [3]. For our study we chose a mountainous terrain in the northwestern part of Argyre basin (44°S – 48.5°S and 323.5°E – 329°E) to reinvestigate the glacial inventory and the history and evolution of glacial landforms and processes in this region with new, higher resolution image data. We produced a detailed morphologic map based on High Resolution Stereo Camera (HRSC) and Context Camera (CTX) imagery. In addition, we analyzed morphologic features with HiRISE and CTX imagery. Here we focus on the morphological map and a more detailed analysis of some possible glacial/periglacial features.

**Morphological map:** The detailed morphological map consists of 13 different units. These units were interpreted as: (1) coarse, blocky terrain, (2) flood basalts, (3) dissected mantle material, (4) intact dust/ice mantle, (5) pingo-like forms, (6) glacier-like flow features, (7) gullies, (8) viscous flow features, (9) “skeleton-terrain”, probably related to sublimation processes within the dust/ice mantle (10) possible large sublimation depressions, (11) polygonal terrains, (12) dunes and (13) mega-ripples (transverse dunes) (Fig. 1).

**Dust-ice mantle:** A smooth and flat mantle interpreted to be a dust/ice mantle [5] (unit 4) occurs in protected depressions or on southern, pole-facing slopes, which receive less insolation. It has a sharp boundary to other units, especially to the coarse, blocky terrain (unit 1), which is often found adjacent to it (Fig. 1). Large areas of the study region consist of flat, partly smooth, partly rougher terrain (unit 3) interpreted to be dissected mantle material.

**Viscous and Glacier-like flow features:** Viscous flow features (unit 8) mostly occur between gullies and on dissected mantle material [6] (Fig. 2a). Often gully debris

fans are superposed on this material. Other locations covered with viscous flow features include dust/ice mantle filled craters, where sediments in inclined craters have been deformed.

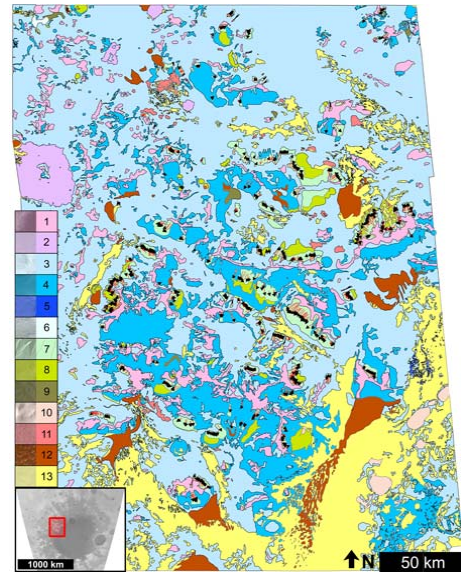


**Figure 1.** Morphologic map of the northwestern Argyre Basin. At the left is the legend (see text for units), in the lower left is a context image of the Argyre Basin (the red square represents the location of the mapping area).

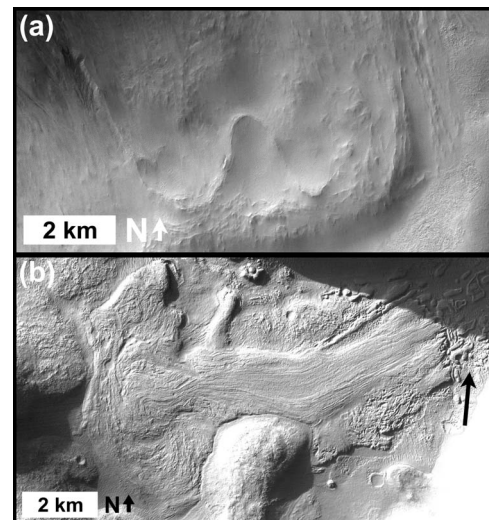


**Figure 2.** (a) Portion of the CTX-Image (P15\_006717\_1329). It shows viscous flow features at a slope, gullies occur north of the area. (b) Portion of the CTX-Image (P19\_008642\_1359). The eastern accumulation area of the glacier-like flow features has been eroded (black arrow).

A well-preserved glacier-like flow feature is located in the northernmost part of the mapping region. (unit 6; Fig. 2b). It shows well developed flow features (striae), which indicate an east to west flow direction with an average gradient of  $\sim 1.9^\circ$ . The glacier is located in a protected area, almost completely surrounded by high mountains.

**Gullies:** Gullies (unit 7), first identified on Mars by [7], are the most common fluvial features in the mapped area. They occur in areas where the mantle appears to be thick and dense. The most obvious characteristics of the gullies are that they only erode into the dust/ice mantle and not the underlying bedrock (Fig. 3a). The preferred orientation of the gullies is on poleward-facing slopes, where the dust/ice mantle is thickest. Often the gullies occur in conjunction with viscous flow features. Stratigraphically the gullies are the youngest landforms in the study region, e.g. superposing transverse dunes (Fig. 3b).

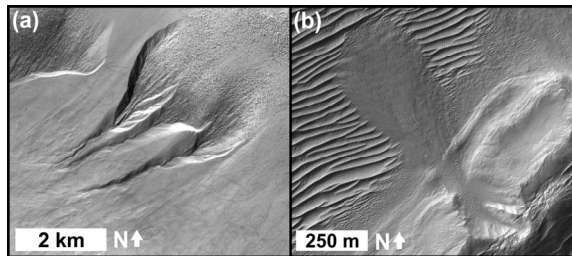


**Figure 3.** (a) CTX-Image (P14\_006638\_1307) which shows a dust-ice mantled hill slope. Large gullies eroded the dust/ice mantle. (b) HiRISE-Image (PSP\_009156\_1335). Here a smaller gully eroded an ice-rich layer (viscous flow feature – unit 8) and is superposed on transverse dunes.

**Pingo-like forms (PLFs):** Pingo-like forms (unit 5) also occur in our study region. PLFs at mid-latitudes were identified and described by [e.g., 8,9]. PLFs appear only in the eastern part of the mapping area. They are located on the flat plains of the Argyre Basin floor. Based on our observations, we have divided the PLFs into two groups: Degraded (cones, central depressions) and non-degraded (domes) PLFs. The degraded PLFs appear closer to the mountain slopes and are found in local topographic depressions, about 40 m below the non-degraded PLFs. The average diameter of degraded PLFs is 170 m and of non-degraded 230 m. They appear to be slightly larger than the PLFs identified by [10], who measured diameters from  $85 \pm 105$  (degraded PLFs) and  $90 \pm 45$  (non-degraded PLFs). Minimum heights of the PLFs, measured with individual Mars Orbiter Laser Altimeter (MOLA) points range from  $\sim 16$  m (degraded PLFs) to  $\sim 25$  m (non-degraded PLFs). However, based only on CTX imagery it is not possible to constrain if the PLFs are really pingos. Even with higher resolution imagery it would be difficult to determine, because different processes can form similar landforms (“equifinality”) [e.g., 11].

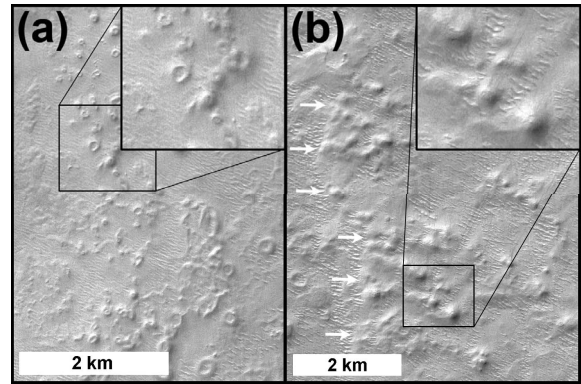


**Figure 4.** (a) degraded PLFs, (b) non-degraded PLFs. The two groups are separated by a 40 m high topographic height difference of the landscape in the western part of (b), next to the PLFs (white arrows). Portions of the CTX-Image (P13-006150\_1323).

**Discussion:** Large areas of the study region are covered with dissected and intact mantle material units. Glacial/periglacial features such as gullies, glaciers and viscous flow features are directly related to the dust/ice layer. All gullies in the study region for example emerged from the dust/ice mantle and are incised into it, indicating a formation by melting of the water-ice-rich mantle [12]. This can also be observed for the viscous and glacier-like flow features which were mobilized by the water/ice rich mantle material like in other mid-latitude regions on Mars [6,13,14] or are related to the dust/ice mantle like the “Skeleton-Terrain”. Other possible glacial landforms such as PLFs and polygonal terrains occur on the dissected mantle material and seem to be exhumed. These landforms might indicate an older glacial period within the Amazonian in this region [1]. Recent studies with HiRISE-data indicate a sequence from glaciation to ablation and perhaps subsequent periglacial processes [3]. We are currently working on the relative and absolute stratigraphy of the different morphologic units in our study region in order to constrain its glacial/periglacial history and evolution.

**References:** [1] Kargel, J. S. and Strom, R. G. (1992) *Geology*, 20, 3-7. [2] Hiesinger, H. and Head, J. W. (2002) *PSS*, 50, 939-981. [3] Banks, M. E. et al. (2008) *JGR*, 113, E12015, doi:10.1029/2007JE002994. [4] Squyres, S. W. and Carr, M. H. (1986) *Science*, 231, 249-252. [5] Mustard et al., (2001) *Nature*, 412, 411-414. [6] Milliken, R. E. et al. (2003) *JGR*, 108, doi:10.1029/2002JE002005. [7] Malin, M. C. and Edgett, K. S. (2000) *Science*, 288, 2330-2335. [8] Dundas, C. M. and McEwen, A. S. (2009) *Icarus*, doi:10.1016/j.icarus.2009.02.020. [9] Burr, D. M. et al. (2009) *PSS*, doi:10.1016/j.pss.2008.11.030. [10] de Pablo, M. A. and Komatsu, G. (2009) *Icarus*, 199, 49-74. [11] King, L. C. (1953) *GSA Bulletin*, 64, 721-752. [12] Christensen, P. R. (2003) *Nature*, 422, 45-47. [13] Head, J. W. et al. (2003) *Nature*, 426, 797-802. [14] Head, J. W. et al. (2005) *Nature*, 434, 346-351.